The 2023 World Congress on
Advances in Structural Engineering and Mechanics (ASEM23)
GECE, Seoul, Korea, August 16-18, 2023

Flexural performance of concrete continuous beams reinforced with FRP bars

Sensen Shi [1)] and *Tiejiong Lou [2)]

[1), 2)] *School of Civil Engineering and Architecture, Wuhan University of Technology, Wuhan 430070, PR China*
[2)] *CEMMPRE, ARISE, University of Coimbra, Coimbra 3030-788, Portugal*
[2)] *loutiejiong@dec.uc.pt*

ABSTRACT

This paper studies the feasibility of replacing steel bars with glass fiber-reinforced polymer (GFRP) and carbon fiber-reinforced polymer (CFRP) bars in RC continuous beams. Firstly, a refined three-dimensional finite element model of a beam is introduced, and the model prediction is compared with the experimental results. Then, a comprehensive numerical study of two-span concrete continuous beams strengthened with steel bars or FRP bars is carried out. The results show that the concrete continuous beams with different FRP bars have a certain moment redistribution ability. ACI-440.1R-15 is too conservative, which completely ignores the bending moment redistribution ability of FRP RC beams, but the beams' sudden brittle failure still needs to be paid attention to. Secondly, due to the lack of yielding of FRP bars, the moment redistribution of FRP RC continuous beams is lower than that of steel RC continuous beams.

1. INTRODUCTION

With the progress of science and technology and the establishment of various large-span and high-rise structures, the reinforced concrete structure has been one of the most widely used structures at present. In the face of its huge use, steel corrosion has also become a problem that people must solve. According to statistics, the degradation of structures and infrastructure caused by corrosion accounts for $ 2.5 trillion per year globally (Wasim 2020). Improving the corrosion resistance of reinforced concrete structures and infrastructure is already the trend of the times. The world, there

[1)] Graduate Student

[2)] Professor

are the following methods to solve the problem of corrosion, using high-performance concrete (Valcuende 2021), cathodic protection (Li 2002), and the use of anti-corrosion coatings (Li 2021). However, these solutions have great shortcomings, the effect is not obvious, the operation is complex or the price is high.

At present, fiber-reinforced polymer (FRP) composite materials are favored by engineers and researchers due to their excellent corrosion resistance and high strength-to-weight ratio. Fiber is a brittle material, which is easy to break and damage. The substrate belongs to a ductile material. The two are glued together and can withstand various effects after drawing and extrusion. FRP bars made of composite materials can replace steel bars and play a role in concrete structures. According to the different fiber materials, FRP bars can be divided into carbon fiber bars (CFRP bars), glass fiber reinforced composite bars (GFRP bars), basalt fiber reinforced composite bars (BFRP bars), and aramid fiber reinforced composite bars (AFRP bars).

Many scholars have studied the bending moment redistribution ability of concrete continuous beams. Chang (2010) et al. studied the method for calculating the ductility coefficient and plastic hinge rotation capacity of flexural members, and compared the plastic hinge rotation capacity specified in the Chinese code, the American code, and the European code within the longitudinal reinforcement ratio range. Ronagh (2015) proposed a probabilistic method to calculate the curvature ductility and allowable bending moment redistribution of beams and introduced a probabilistic model. Ehsani (2019) et al. studied the flexural behavior of two-span RC beams. They found that using high-performance fiber-reinforced concrete (HPFRCC) and reducing stirrup spacing can improve components' ultimate bearing capacity and bending moment redistribution capacity. Tian (2022) et al. used the stiffness method to calculate the moment redistribution coefficient of the beam at the key section and obtained the conclusion that the moment redistribution coefficient at the mid-span is linearly related to the height of the compression zone.

In this paper, the two-span RC continuous beam is taken as the research object. The main research variables are the types of reinforcement bars, which are steel bars, CFRP bars, and GFRP bars. The finite element analysis software ABAQUS was used to model and conduct a comprehensive numerical study to explore the flexural performance of concrete continuous beams under different reinforcement bars.

2. MODEL PREDICTION

2.1 Model

The model is established by using the simply supported beam in the test of Huang et al. (Huang 2021). The beam span is 1250 mm and the beam section is 150 mm × 200 mm, as shown in Fig. 1. The thickness of the protective layer is 25 mm. Two BFRP bars with a diameter of 10 mm are set at the top and bottom of the beam, and stirrups are BFRP bars with a spacing of 100 mm and a diameter of 10 mm. The tensile strength,

elastic modulus, and elongation of BFRP bars are 1200 MPa, 55 GPa, and 0.02, respectively.

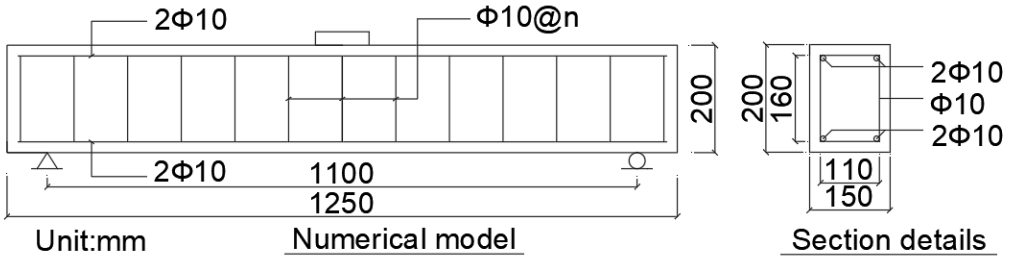

Fig. 1 Simple test beams (schematic diagram)

2.2 Constitutive Relation

The finite element model is modeled by ABAQUS. The plastic damage model is used to describe the damage and cracking of concrete materials. Two damage factors, namely tensile damage and plastic damage, are introduced to further study the mechanical properties of concrete. The eight-node reduced integral three-dimensional solid element (C3D8R) is used for concrete, and the two-node linear three-dimensional bar element (T3D2) is used for steel bars and FRP bars in the beam.

When modeling, under the premise that the model can accurately reflect the real stress situation of the structure, the simpler the model is, the better. To simplify the mechanical model reasonably, this paper makes the following assumptions:

(1) Concrete obeys the principle of small deformation, ignoring its shrinkage and creep;

(2) Ignoring the relative slip between the steel bar and the concrete, the “Embedded” implant technology is adopted, that is, the deformation of the steel bar and the attached concrete is considered to be the same;

(3) In this numerical simulation, the connection between the bearing and the FRP material is “Tie”;

Considering the nonlinearity of the material, the material law introduced in the finite element model is shown in Fig. 2.

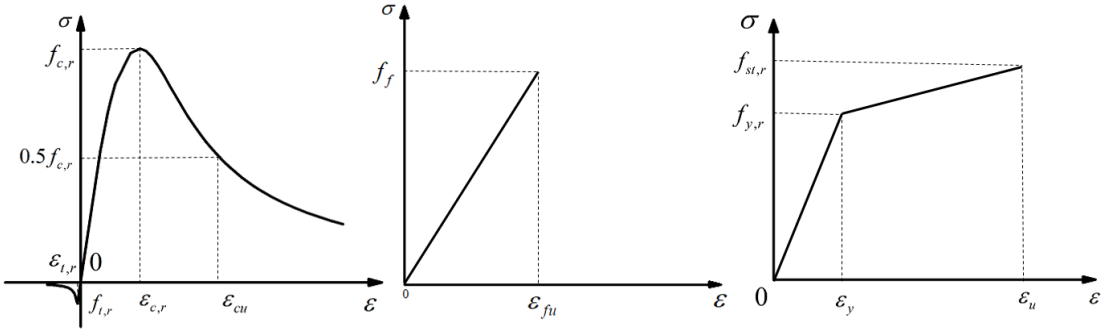

Fig. 2 Material stress-strain curves (a) Concrete under compression and tension; (b) FRP bars; (c) Steel bars

where σ represents stress, ε represents strain, $f_{c,r}$ is the representative value of uniaxial compressive strength of concrete, $\varepsilon_{c,r}$ is the peak compressive strain of concrete corresponding to the uniaxial compressive strength $f_{c,r}$; $f_{y,r}$ is the yield strength representative value of the steel bar, $f_{st,r}$ is the ultimate strength representative value of the steel bar, ε_y is the yield strain of the steel bar corresponding to $f_{y,r}$, and ε_u is the peak strain of the steel bar corresponding to $f_{st,r}$; f_f and ε_f are the fracture strength and strain of FRP bars.

2.3 Comparative Experimental Data

Based on the above material parameters, the model prediction is compared with the experimental results after the model is established: the load-deflection curve and load-strain curve. The model prediction is consistent with the corresponding experimental observation results, as shown in Fig. 3, which proves the feasibility and reliability of the above modeling method and can be used as the basis for subsequent research.

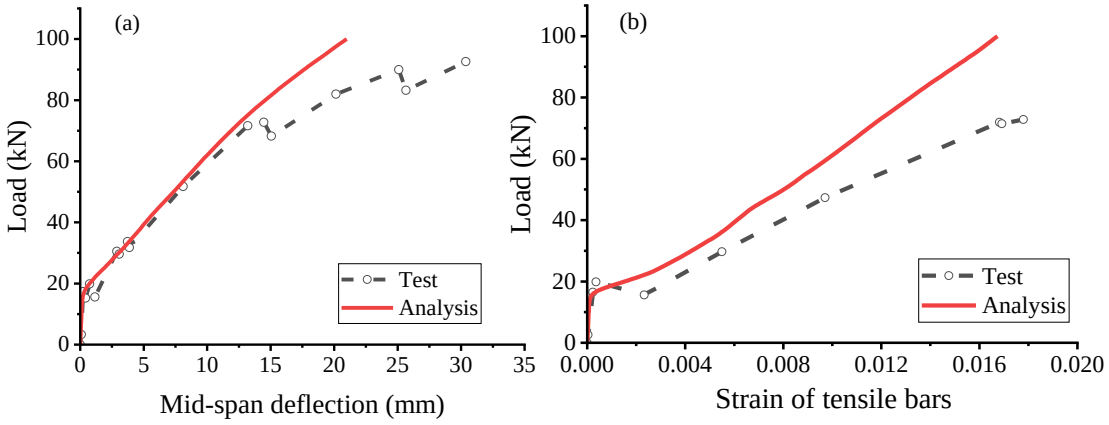

Fig. 3

Comparison between numerical and test results. (a) load-displacement; (b) load versus strain in tensile bars

3. RESULTS AND DISCUSSION

Three two-span concrete continuous beams were tested, which were symmetrically applied to each span under the central point load, as shown in Fig. 4 and Fig. 5 The total length of the beam is 10090mm, the length of the inner bar is 10040mm, and the section of 500mm × 300mm is adopted. The research variables are the type of reinforcement bars (steel, CFRP, GFRP).

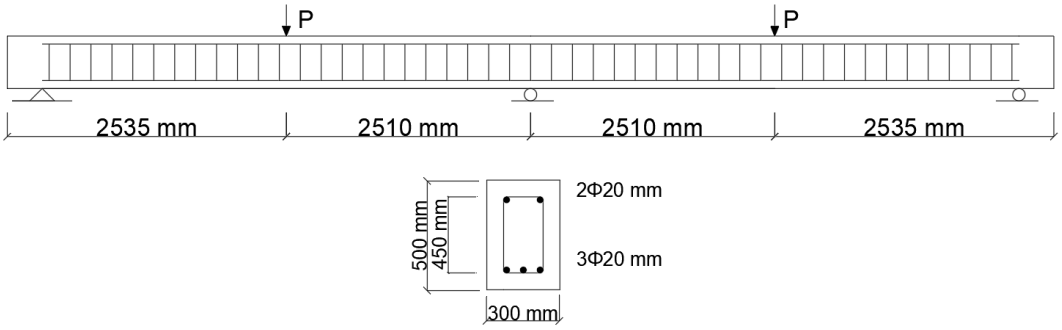

Fig. 4 RC continuous beams for numerical evaluation (schematic diagram)

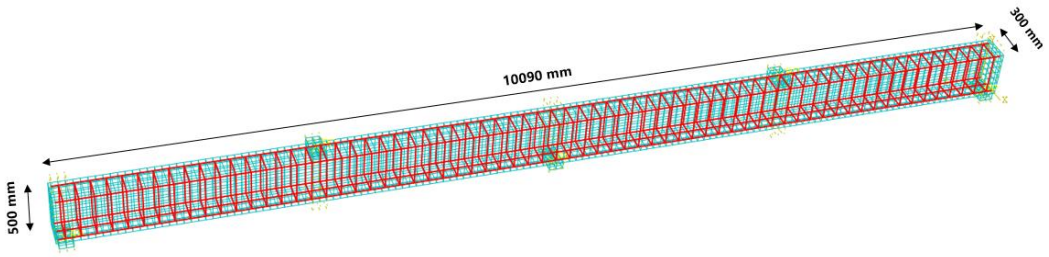

Fig. 5 ABAQUS finite element mesh of concrete continuous beams with FRP bars

The concrete strength of the RC continuous beam is c30, and the three beams are set with two inner bars with a diameter of 20 mm at the top and three inner bars with a diameter of 20 mm at the bottom. The stirrups with a spacing of 150 mm and a diameter of 10 mm are used. The types of reinforcement bars of each concrete continuous beam are shown in Table 1.

Table 1 Material properties of steel and FRP bars

Material	*d/mm*	*fy / MPa*	*fu / MPa*	*E / GPa*
Steel	20	485	625	200
Stirrup	20	300	480	190

GFRP	20	-	700	46
CFRP	20	-	1800	150

3.1 Load–Deflection Behavior

Fig. 6 shows the load-deflection behavior of three experimental beams from loading to failure. In the first stage of the stress of the concrete continuous beam, the three beams all show linear response. At this time, the whole section of the beam participates in the work, and the reinforcement bars and the concrete are jointly stressed. At this stage, the internal force of the beam is small, so the cracking load of the three beams is not much different, and the deflection is small. As the load increases, the beam enters the second stage after cracking. Because the strength of the steel bars is higher than that of the FRP bars, the curve of the beam with steel bars is higher than the curve of the FRP bars, with the increase of load, the stress process of the steel RC continuous beam enters the third stage. The load-deflection curve of FRP concrete continuous beams is only composed of two stages due to the non-yield stage of FRP bars. Finally, the brittle failure of FRP concrete continuous beams occurs.

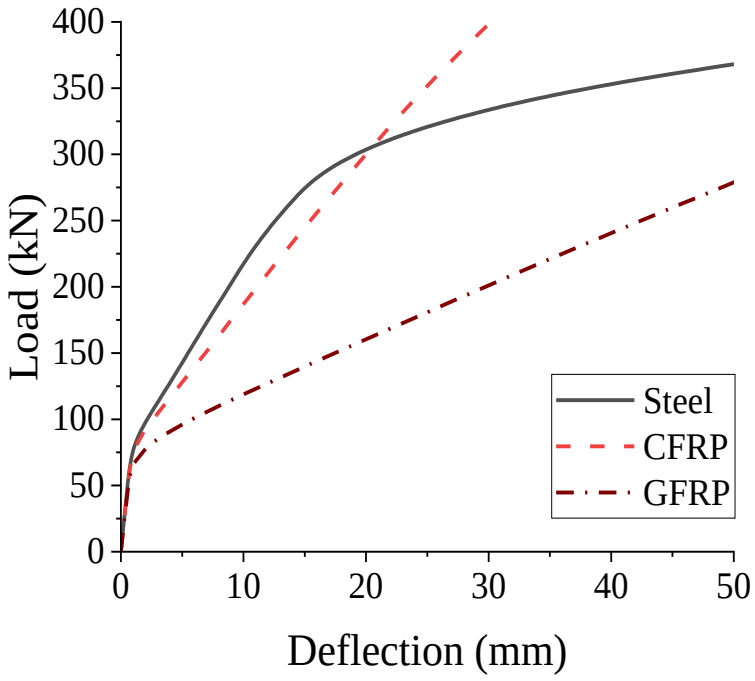

Fig. 6 Load–deflection curves

The failure of the three beams occurs when the critical section strain of the concrete reaches the ultimate compressive strain of 0.0035. At this time, the ultimate deflection of the RC continuous beam is 54 mm, while the CFRP concrete continuous beam is 51 mm, which is 57 % lower than that of the GFRP concrete continuous beam. This is because CFRP bars have higher elastic modulus than GFRP bars, as the load

increases, the mid-span displacement of the CFRP concrete beam increases more slowly with the load.

3.2 Loading-Strain

Fig. 7 shows the load-strain relationship of the reinforcement bars at the critical section (mid-span section and center support section), which is divided into top force bars and bottom force bars. With the increase of the load, the load-strain curve of the steel bars is mainly divided into three stages, while the FRP bars have only two stages due to the material properties.

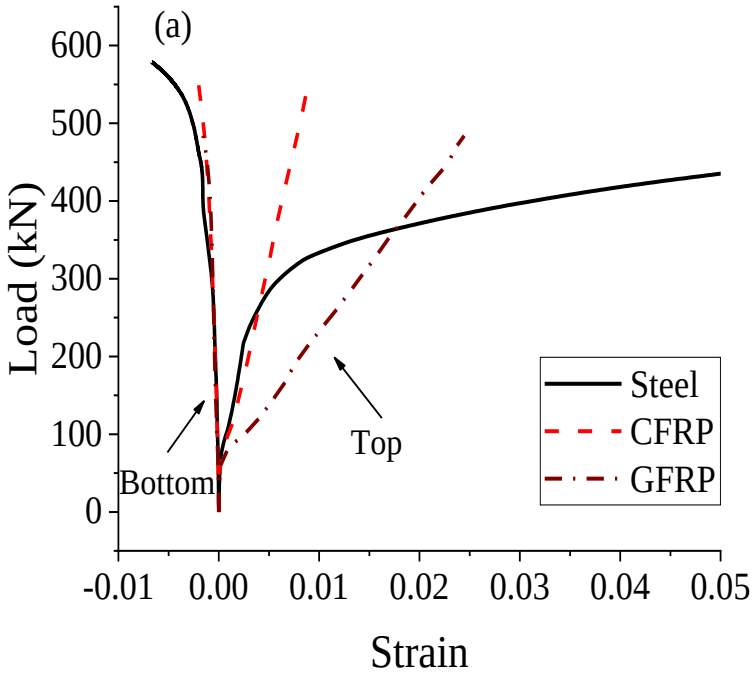

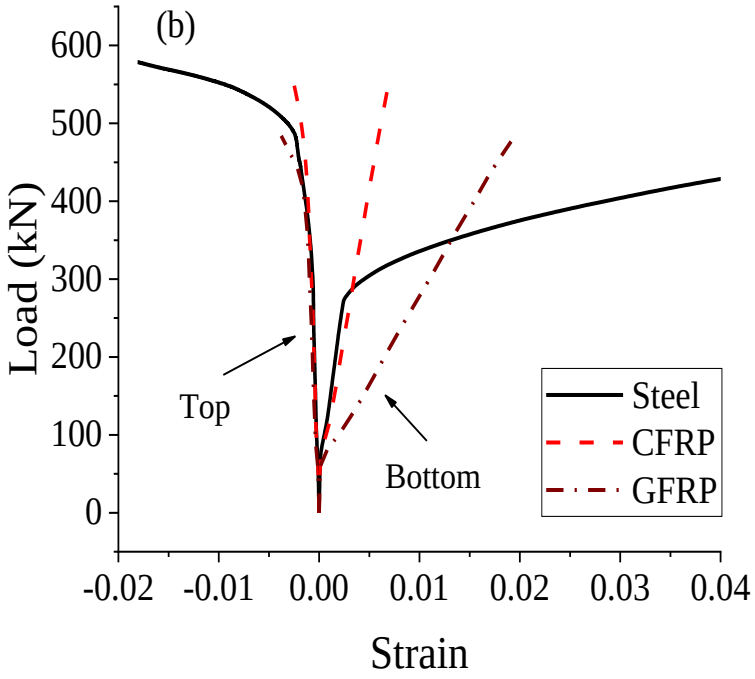

Fig. 7 Load versus reinforcement bar strain curves: (a) the section at the center support; (b) the mid-span cross-section

In the stage where the concrete is not cracked, it is mainly the concrete that provides the bearing capacity, and the stress and strain of the internal steel bars are small. When the first crack occurs, the force originally borne on the concrete suddenly transfers to the reinforcement bars, resulting in a sudden change in the force of the reinforcement bars and a sharp increase in strain. As the steel bars yield, the slope of the line decreases, but the image slope of the FRP bars remains unchanged. When the beam fails, the strain measured in the top steel bars at the middle support section is about 1.3 times that measured in the bottom steel bars at the mid-span section.

3.3 The Development of Reaction Force and Bending Moment

Fig. 8 is the load-reaction curve of the three beams at the middle support and the end support. It can be seen from Figure 7 that although the reinforcement bars forms are different, the reaction forces at the two different supports are roughly the same, and the reaction forces at the middle support are always higher than the reaction forces at the end support.

Fig. 9 shows the bending moment-load curve of three continuous beams at the critical sections (middle support section and mid-span section). When the loads are small, the bending moments at the middle support section are larger than that at the mid-span section. However, with the increase of load, cracks will gradually occur at the center support and accompanied by the generation of plastic hinges, so that the bending moments will be redistributed from the center support to the mid-span section. It can be

seen from the diagram that when the load reaches 250 kN, the slope of the curve will change greatly due to the redistribution of the bending moment.

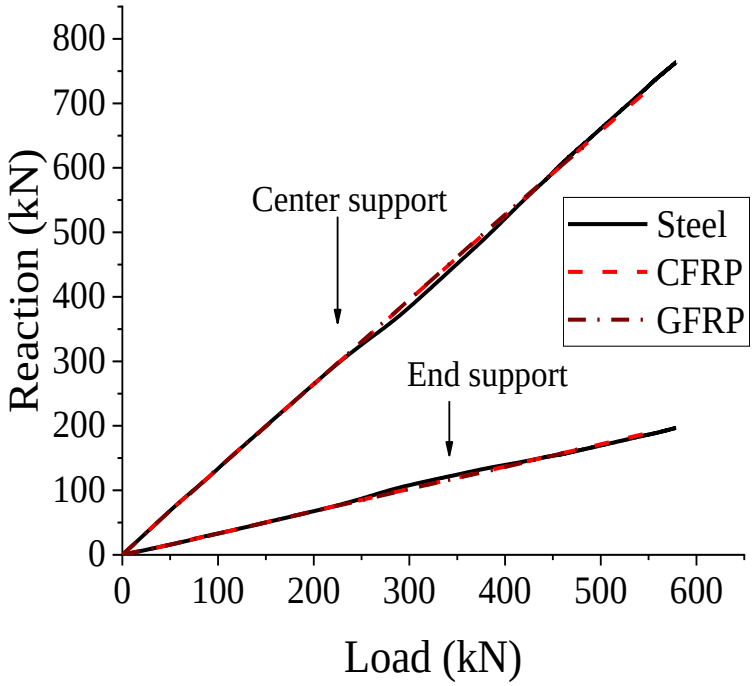

Fig. 8 Load-reaction curves

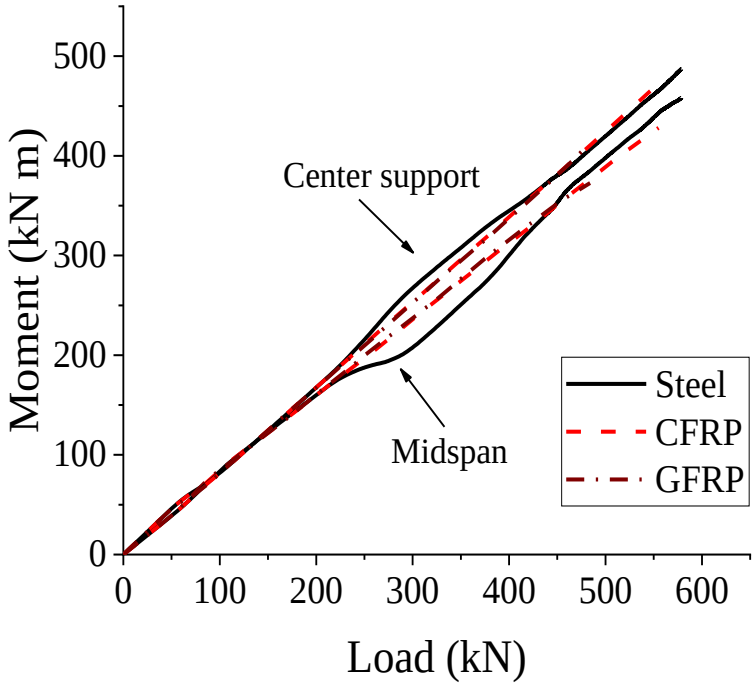

Fig. 9 Moment-load curves

3.4 Moment Redistribution

The elastic bending moment of the cross-section of the three continuous beams simulated above is 0.156 FL at the mid-span and 0.188 FL at the center support, where F and L are the load applied at the mid-span and the span of the beam, respectively, as shown in Fig. 10. It should be noted that the above bending moment values are calculated based on the uniform bending stiffness along the beam span. However, the occurrence of concrete cracks under different load levels reduces the bending stiffness of beams at different positions, so the moment distribution also changes.

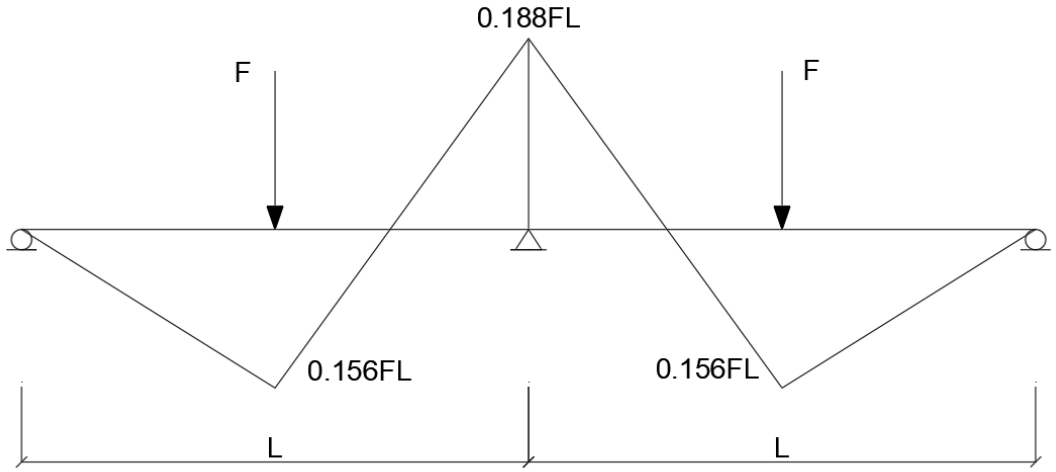

Fig. 10 Elastic moment distribution assuming constant Bending stiffness

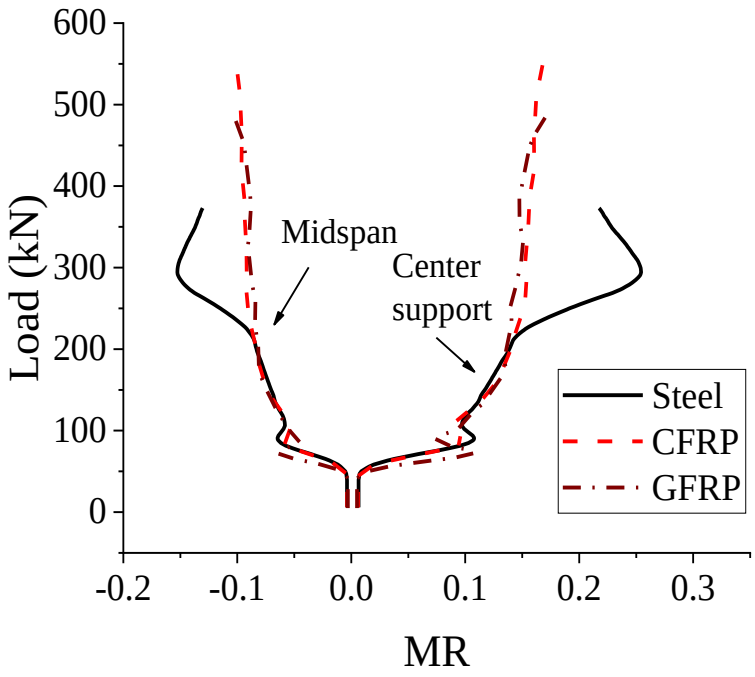

Fig. 11 Moment redistribution-load curve

Fig. 11 shows the law of moment redistribution of three concrete continuous beams with different reinforcement bars with the change of external load. Before the concrete cracks, the moment redistribution of the three concrete continuous beams does not change. After the concrete cracks, the moment redistribution of the structure increases rapidly. For concrete continuous beams with steel bars, the moment redistribution is similar to that of FRP bars before the steel bars yield. With the steel bars in the beam at the center support gradually entering the yield state, the bending moment of the section at the center support is rapidly distributed to the mid-span section. It can be seen from the diagram that when the load reaches 200 kN, the moment redistribution of the RC continuous beam at the two critical sections increases rapidly. After that, due to the change of relative stiffness in the beam after the yield of the steel bars, the evolution trend of moment redistribution changes, and the degree of moment redistribution is gradually reduced. For FRP RC continuous beams, the redistribution of bending moment in the beam will gradually stabilize, but it is always lower than that of steel RC continuous beams. This is due to the linear elastic characteristics of FRP bars, and plastic hinges will not be formed in FRP-reinforced members. At the same time, the moment redistribution of GFRP RC continuous beams is always lower than that of CFRP RC continuous beams at this stage. This is because the elastic modulus of GFRP bars is low, and the last two beams are finally destroyed along with the moment redistribution process.

According to norms, the moment when the ultimate compressive strain of concrete in the mid-span is 0.0035 is taken as the ultimate bending moment, and the ultimate bending moment at the critical section is calculated by the measured reaction force. By comparing the elastic bending moment and the ultimate bending moment when the concrete continuous beam is destroyed, as well as the bending moment bearing capacity of the critical sections, the redistribution of the bending moment is evaluated. The moment redistribution factor MR from one critical section to another can be obtained from Eq. (1).

$$MR\% = \frac{M_e - M_u}{M_e} \times 100 \tag{1}$$

where M_e and M_u are the critical section elastic bending moment and ultimate bending moment at failure. The elastic bending moment, ultimate bending moment, and moment redistribution coefficient of the critical sections of the three continuous beams at the mid-span and center support are shown in Table 2.

Table 2 Moment redistribution coefficient

Beam	Elastic bending moment (kN m)	Ultimate bending moment (kN m)	Moment redistribution

					coefficient(%)	
	Midspan	Middle support	Midspan	Middle support	Midspan	Middle support
Steel	290.98	350.66	320.17	270.95	-10.0	22.7
CFRP	433.03	521.86	472.91	428.23	-9.2	17.9
GFRP	377.64	455.10	412.65	372.96	-9.3	18.0

According to Table 2, the ultimate bending moment of three concrete continuous beams at the mid-span support section will be less than the predicted elastic bending moment, while the ultimate bending moment at the mid-span section will be higher than the predicted elastic bending moment. This is because the moment redistribution occurs so that the bending moment is redistributed from the center support section to the mid-span section. This result also shows the feasibility of replacing steel bars with FRP bars in continuous beams. ACI-440.1R-15 (2006) stipulates that it is too conservative to completely ignore the moment redistribution ability of FRP bars. In addition, for the concrete continuous beam with steel bars, the moment redistribution coefficient will be higher than the other two beams due to the steel bars' yield characteristics, so the beam has greater ductility in the plastic hinge region. The moment redistribution coefficient at failure is close for two FRP RC continuous beams.

4. CONCLUSIONS

In this paper, refined three-dimensional finite element models are established. By studying concrete continuous beams with different reinforcement bars, the possibility of replacing steel bars with FRP bars and the flexural performance of continuous beams are explored. The conclusions are as follows:

1. FRP RC continuous beams can be a certain degree of moment redistribution, reflecting the feasibility of using FRP bars instead of steel bars. ACI-440.1R-15 regulation does not consider the moment redistribution of continuous beam members with FRP bars as too conservative.
2. Due to the lower elastic modulus of GFRP bars, the moment redistribution of GFRP RC continuous beams is always lower than that of CFRP RC continuous beams in the stage of stable redistribution of bending moment.
3. Compared with RC continuous beams, FRP concrete continuous beams' bending moment redistribution coefficient is lower due to the lack of yield.
4. After the steel bars yield, the relative stiffness in the continuous beam changes, which leads to the change in the evolution trend of the moment redistribution, and the moment redistribution will decrease.

ACKNOWLEDGMENT

The work has been supported by the Portuguese Foundation for Science and Technology under Grants No. 2022.04729.CEECIND, UIDB/00285/2020 and LA/P/0112/2020.

REFERENCES

Wasim, M., Ngo, T. D. and Abid, M. (2020), “Investigation of long-term corrosion resistance of reinforced concrete structures constructed with various types of concretes in marine and various climate environments,” *Construction and Building Materials*, 237, 117701.

Valcuende, M., Lliso-Ferrando, J. R., Ramón-Zamora, J. E. and Soto, J. (2021), “Corrosion resistance of ultra-high performance fibre-reinforced concrete,” *Construction and Building Materials*, 306, 124914.

Li, Z., Gan, F. and Mao, X. (2002), “A study on cathodic protection against crevice corrosion in dilute NaCl solutions,” *Corrosion Science*, **44**(4), 689-701.

Li, Z., Ravenni, G., Bi, H., Weinell, C. E., Ulusoy, B., Zhang, Y. and Dam-Johansen, K. (2021), “Effects of biochar nanoparticles on anticorrosive performance of zinc-rich epoxy coatings,” *Progress in Organic Coatings*, 158, 106351.

Huang, Z., Chen, W., Hao, H., Chen, Z., Pham, T. M., Tran, T. T. and Elchalakani, M. (2021), “Flexural behavior of ambient cured geopolymer concrete beams reinforced with BFRP bars under static and impact loads,” *Composite Structures*, 261, 113282.

Chang, Y. Y. and Gong, J. X. (2010), “Ductility and moment redistribution of reinforced concrete flexural members,” *Jianzhu Kexue Yu Gongcheng Xuebao (Journal of Architecture and Civil Engineering)*, **27**(2), 38-44.

Ronagh, H. R. (2015), “Probabilistic models for curvature ductility and moment redistribution of RC beams,” *Computers and Concrete, An International Journal*, **16**(2), 191-207.

Ehsani, R., Sharbatdar, M. K. and Kheyroddin, A. (2019), “Ductility and moment redistribution capacity of two-span RC beams,” *Magazine of Civil Engineering*, (**6** (90)), 104-118.

TIAN, X., SHI, P. F., DING, S. S., MIAO, H. B. and ZHEN, Bin. (2022), “T-Section beams strengthened with fiber reinforced polymer,” *Research &Explore* **40**(3), 36-42.

ACI Committee 440. Guide for the Design and Construction of Structural Concrete Reinforced with FRP Bars; ACI 440.1R-06; American Concrete Institute: Farmington Hills, MI, USA, 2006.